Eur. Phys. J. C 53, 257–265 (2008)
DOI 10.1140/epjc/s10052-007-0452-y

THE EUROPEAN PHYSICAL JOURNAL C

Regular Article – Theoretical Physics

A complete one-loop description of associated tW production at LHC and an estimate of possible genuine supersymmetric effects

M. Beccaria[1,2], C.M. Carloni Calame[3], G. Macorini[4,5], G. Montagna[6,7,a], F. Piccinini[6,7], F.M. Renard[8], C. Verzegnassi[4,5]

[1] Dipartimento di Fisica, Università del Salento, Italy
[2] INFN, Sezione di Lecce, Italy
[3] School of Physics & Astronomy, Southampton University, UK
[4] Dipartimento di Fisica Teorica, Università di Trieste, Italy
[5] INFN, Sezione di Trieste, Italy
[6] Dipartimento di Fisica Nucleare e Teorica, Università di Pavia, Italy
[7] INFN, Sezione di Pavia, Via A. Bassi 6, 27100 Pavia, Italy
[8] Laboratoire de Physique Théorique et Astroparticules, Université Montpellier II, France

Received: 18 June 2007 / Revised version: 2 October 2007 /
Published online: 10 November 2007 –

Abstract. We compute, in the MSSM framework, the sum of the one-loop electroweak and of the total QED radiation effects for the process $pp \to tW + X$, initiated by the parton process $bg \to tW$. Combining these terms with the existing NLO calculations of SM and SUSY QCD corrections, we analyze the overall one-loop supersymmetric effects on the partial rates of the process, obtained by integrating the differential cross section up to a final variable invariant mass. We conclude that, for some choices of the SUSY parameters and for relatively small final invariant masses, they could reach the relative ten percent level, possibly relevant for a dedicated experimental effort at LHC.

PACS. 12.15.Lk; 12.38-t; 13.75.Cs; 14.80.Ly

1 Introduction

Single top production at LHC has already been emphasized by several authors [1, 2] as one of the processes to be possibly measured with maximal experimental accuracy. The main and known reason is the fact that in the standard model from this measurement one would be able to derive the first direct determination of the Wtb coupling V_{tb}, assumed to be practically equal to one if unitarity of the CKM matrix is postulated. Since the rates of the three different single top production processes, usually called t-channel, s-channel, and associated production, are proportional to $|V_{tb}|^2$, an accurate measurement of those rates would correspond, in principle, to a correspondingly accurate measurement of V_{tb}. From the preliminary experimental analyses [3–5] one hopes that a realistic overall accuracy might eventually reach the ten percent size. The corresponding precision of the determination of V_{tb} would therefore be of the order of five percent, if no extra theoretical uncertainties had to be added.

The previous statement requires a description of the status of the existing theoretical calculations. A complete NLO QCD calculation exists for all the three single top processes in the standard model [6–14] with an attached uncertainty that varies with the process. It seems probable that this uncertainty will be essentially reduced by the future LHC related measurements, and we shall return to this point later on in the paper. For the three production channels, SUSY NLO QCD effects have recently been evaluated in the MSSM [15]. The pure electroweak one-loop effects in the MSSM have been computed recently for the case of associated tW production [16]. This calculation did not contain, though, the QED radiation corrections. In the case of the total rate, a modest (few percent) relative effect was found. In a subsequent note [17] it was shown that, still at the pure electroweak one-loop level, more interesting effects could be found from the measurement of partial rates, defined as an integral of the differential cross section performed from threshold to a final suitable invariant mass. In particular, for low values of the latter, a positive effect was computed that obviously could not be due to a violation of the CKM matrix structure leading to smaller values of V_{tb}.

Starting from these premises, the purpose of this paper is to provide a really "complete" calculation of one-loop effects in the MSSM on the partial rates of the tW production process, where for each partial rate the QED effect is also included. Moreover, we shall provide a preliminary evaluation of the overall theoretical uncertainties taking

[a] e-mail: guido.montagna@pv.infn.it

into account the variation of the final considered invariant mass. The result will be, essentially, an indication of an "optimal" choice of partial rate, i.e. of one for which the two combined requests of maximal electroweak effect and of minimal overall uncertainty might be satisfied. This could lead to a relevant precision test of the MSSM at LHC, whose accuracy would certainly improve with time if preliminary encouraging signals were revealed, motivating more accurate dedicated experimental measurements.

The paper will be organized in the following way: Sect. 2 will contain a review of the electroweak calculation, essentially shortened since all the necessary details have already been given in [16]. In Sect. 3, the new calculation of the additional QED radiation effect will be described. Section 4 will contain a brief discussion of the existing QCD calculations and of their uncertainties, taking into account the considered variation of the final invariant mass. Summarized results will be discussed in Sect. 5 and a few conclusions will finally appear in Sect. 6.

2 Electroweak one-loop effects

At the partonic level the associated tW^- production is initiated by the process $bg \to tW$, described at Born level by the two diagrams in Fig. 1.

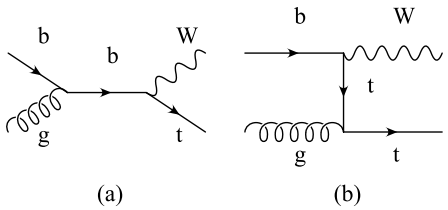

Fig. 1. Born diagrams for the process $bg \to tW^-$

In a previous paper [16], we have analyzed the complete one-loop electroweak corrections to this process treating QED effects in the soft-photon approximation. Here, we summarize briefly the results of [16] as a background to the complete analysis including hard QED radiation to be discussed in the remaining part of the present paper.

Our starting observable for this process was the invariant mass distribution defined by

$$\frac{\mathrm{d}\sigma(pp \to tW^- + X)}{\mathrm{d}M_{tW}} = \int \mathrm{d}x_1\,\mathrm{d}x_2\,\mathrm{d}\cos\theta[b(x_1,\mu)g(x_2,\mu)+g(x_1,\mu)b(x_2,\mu)] \times \frac{\mathrm{d}\sigma_{bg\to tW^-}}{\mathrm{d}\cos\theta}\delta\big(\sqrt{x_1x_2S}-M_{tW}\big)\,, \quad (1)$$

where $\sqrt{S}$ is the proton–proton c.m. energy, M_{tW} is the tW invariant mass, θ is the top-quark scattering angle in the partonic c.m. frame, and $i(x_i,\mu)$ are the distributions of the parton i inside the proton with a momentum fraction x_i at the scale μ.

The invariant mass distribution $\mathrm{d}\sigma/\mathrm{d}M_{tW}$ has been evaluated for a number of SUSY benchmark points with a wide variation of mass spectra and values of the mixing parameter $\tan\beta$. In particular, the considered MSSM points have been the standard ATLAS DC2 SU1 and SU6 [18] and two generic mSUGRA points with light spectrum. The calculation has been performed with a kinematical cut on the W or top transverse momentum $p_{\mathrm{T,min}} = 15$ GeV, and we have included a QED soft-photon contribution, computed assuming an upper value of the soft-photon energy $\Delta E = 0.1$ GeV. The main results of our detailed numerical investigation can be summarized as follows. The electroweak one-loop effect in the MSSM is the sum of the pure SM and of the genuine SUSY components. These two terms have a fundamentally different dependence on the invariant mass of the final state. More precisely, the SM

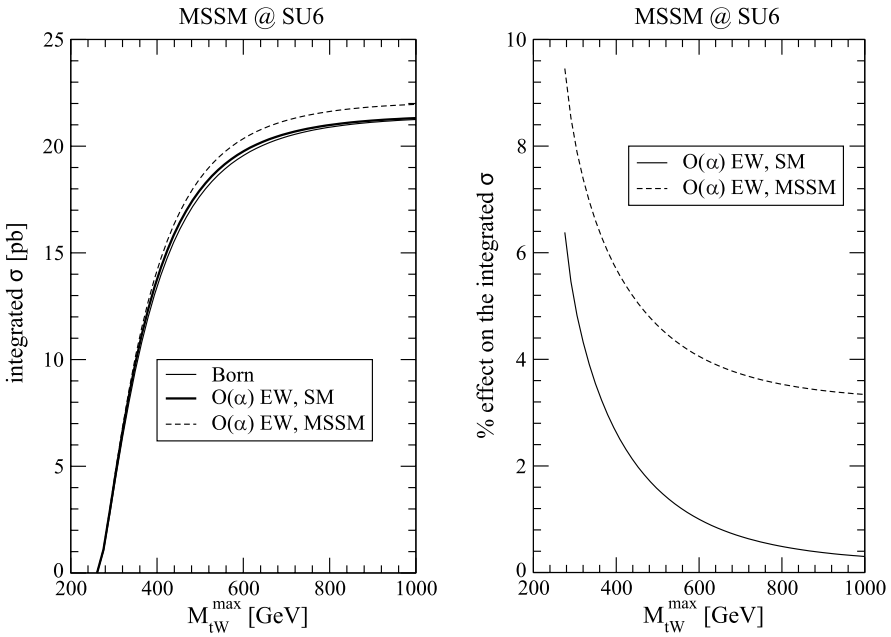

Fig. 2. Integrated cross section (from threshold up to $M_{tW}^{\max}$) in the soft-photon approximation

effect varies from positive values of approximately 5% in the lowest invariant mass range to larger negative values in the high invariant mass sector. One actually expects from general considerations such negative effects, coming from a logarithmic contribution of Sudakov kind to the asymptotic value of the scattering amplitude. As a consequence of the change of sign of the SM contribution, the overall effect in the total rate is practically vanishing. The genuine SUSY effect has a rather different nature. It remains systematically positive in the whole invariant mass range (realistically considered up to a final value of 1 TeV) for all the considered SUSY benchmark points, assuming essentially the same relative effect of 3%–4% in all cases, with a maximum value reached in the SU6 point. The lack of a negative large energy effect can be understood as a consequence of the fact that in the considered benchmark points there are relatively large SUSY masses that appear in the virtual loops, which hides the appearance of asymptotic logarithmic Sudakov effects. A possibility that was considered in the note [17] is that of considering partial rates, in particular low energy partial rates, obtained by integrating the differential cross section from threshold to a given final invariant mass. If the latter is fixed at small but meaningful values (say, 400 GeV), the relative SM and genuine SUSY effects sum up. Also, the effect will be positive, therefore not possibly due to those vio-

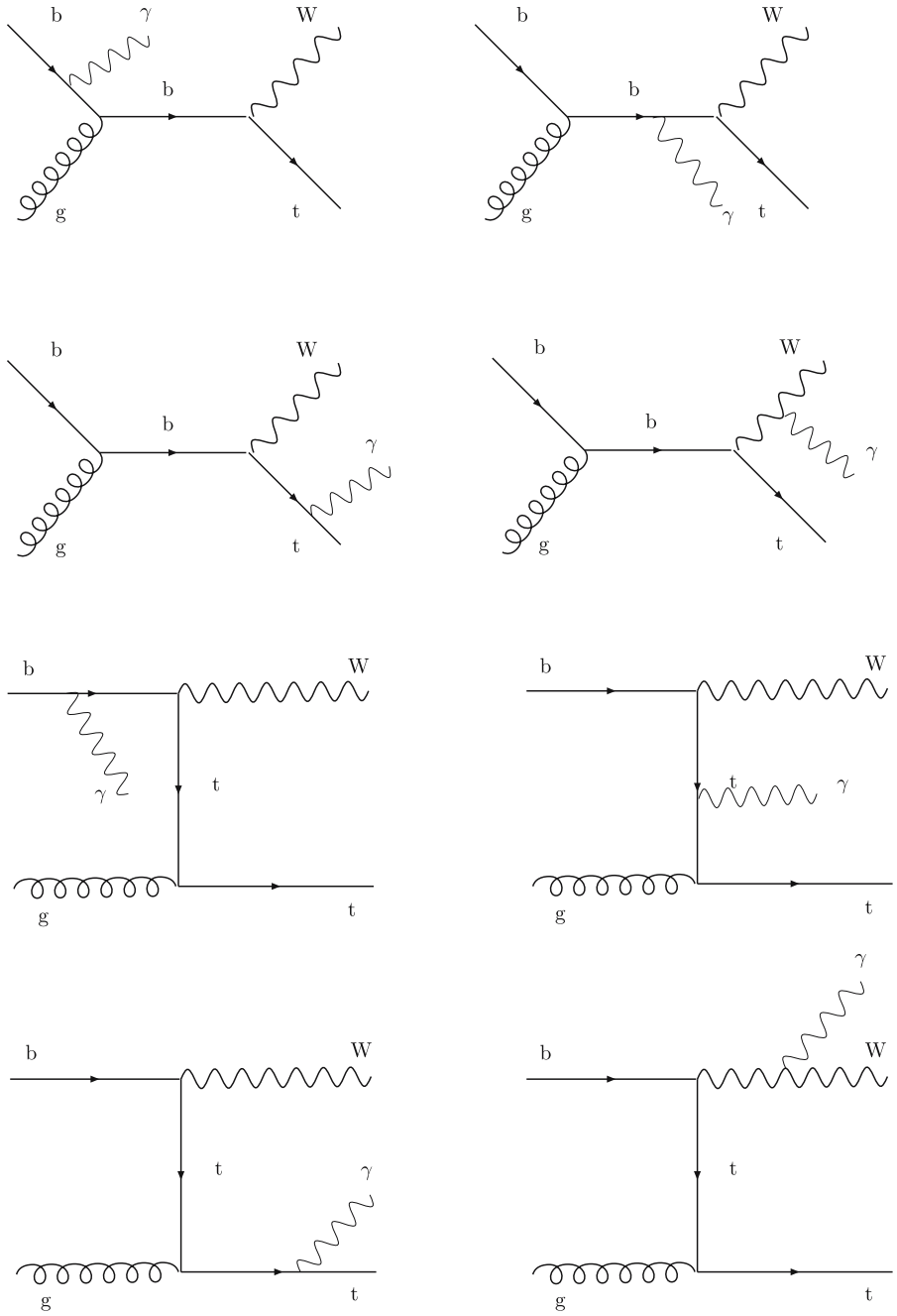

Fig. 3. Diagrams for the radiative process $bg \to tW^-\gamma$

lations of the CKM matrix structure that would decrease the value of V_{tb}. This idea is confirmed by the detailed numerical calculation, shown in Fig. 2 taken from [17] and computed with the same kinematical and infrared cuts as in [16]. One sees that for values of the final invariant mass in the range mentioned above the MSSM electroweak effect is not negligible, reaching values of 6%–7%, that appear possibly relevant.

The previous considerations miss two important points. The first one is an original calculation of the complete (soft and hard) QED effect, which has never been performed before. The second one is a summary of the QCD NLO calculations, including both SM and SUSY QCD (the latter will be in fact rather useful for our purposes). These two topics will be discussed in the forthcoming sections.

3 QED radiation

The $\mathcal{O}(\alpha)$ electroweak corrections include contributions from virtual and real photon emission. The virtual photon exchange diagrams belong to the complete set of electroweak virtual corrections and are necessary for the gauge invariance of the final result. The singularities associated with the massless nature of the photon have been regularized by introducing a small photon mass m_γ. The real radiation contribution has been split into a soft part, derived within the eikonal approximation, where the photon energy has been integrated from the lower bound m_γ to a maximum cut off ΔE, and into a hard part, evaluated by means of a complete calculation of the Feynman diagrams relative to the radiative process $bg \to tW^-\gamma$ shown in Fig. 3. The soft real contribution contains explicitly the photon mass parameter m_γ. The logarithmic terms containing m_γ cancel exactly in the sum of virtual and soft real part, leaving only polynomial spurious terms, which approach zero at least as m_γ^2. The hard contribution, integrated from the minimum photon energy ΔE to the maximum allowed kinematical value, can be calculated with a massless external photon. The complete matrix element for real radiation, including fermion and W mass effects, has been calculated analytically with the help of FORM [19], in order to compute automatically the traces of strings of Dirac matrices. As an internal check, the complete matrix element has been verified to recover (in the limit $k \to 0$, where k stands for the photon momentum) the analytical expression of the eikonal approximation, factorized over the tree-level amplitude, as given in [20].

The integration over the phase space has been performed numerically with Monte Carlo methods. In order to treat efficiently the regions related to the infrared and collinear singularities, the importance sampling technique has been adopted. In particular, the photon energy is generated in the partonic c.m. system according to the behaviour $1/E_\gamma$; the photonic angular variables are generated with a multi-channel strategy according to the distribution $1/(1-\beta_i \cos\vartheta_{\gamma i})$, where $i = b, t, W$, β_i represents the velocity of the i particle, and $\vartheta_{\gamma i}$ is the relative angle between the photon and the emitting charged particle i.

The final cross section has to be independent of the fictitious separator ΔE, for sufficiently small ΔE values. This has been checked numerically to hold at the level of few 0.01% for $\Delta E \leq 1\,\text{MeV}$, as shown in Fig. 4 (right panel), despite the strong sensitivity to ΔE of the soft plus virtual and of the hard cross section separately, as shown in Fig. 4 (left panel). The leading logarithmic dependence on ΔE (with opposite coefficients) in the soft plus virtual and in the hard cross sections is manifest in the logarithmic scale plot.

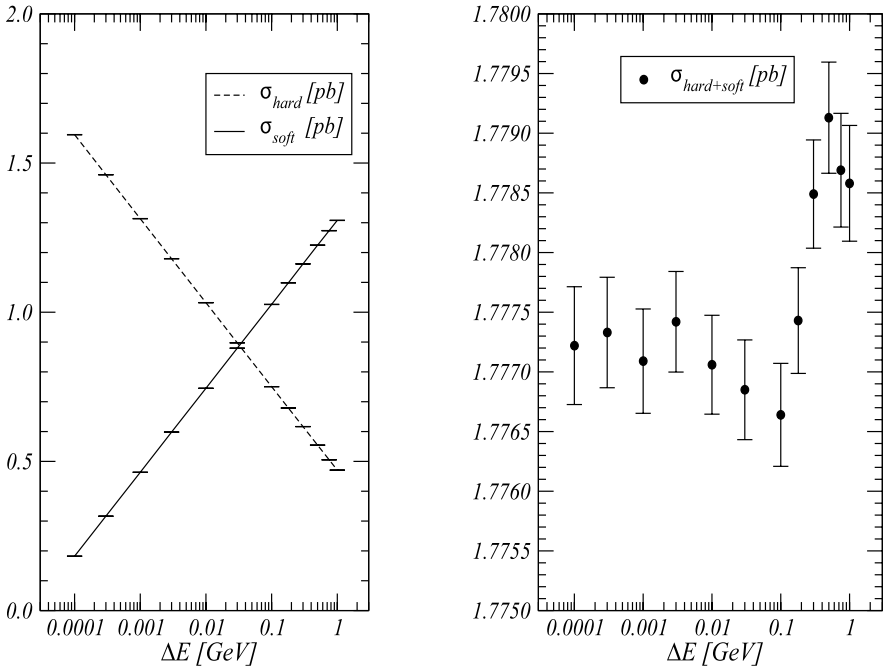

Fig. 4. *Left*: dependence of the $\mathcal{O}(\alpha)$ soft plus virtual and hard cross sections on the soft–hard separator ΔE. *Right*: independence of the sum of $\mathcal{O}(\alpha)$ soft plus virtual and hard cross sections of the separator ΔE, checked numerically up to an accuracy of the order of 0.01%

4 QCD effects

4.1 NLO SM corrections

The NLO SM QCD corrections to the tW signature have been calculated by various authors [21–24] within the on-shell approximations for W-boson and top quark. In [24] the corrections considering also the decay of the top quark have been evaluated. Such a calculation is implemented in the fixed-order Monte Carlo program MCFM [25], v5.1, which we use to estimate the QCD uncertainties associated with the integrated tW mass distribution. In our simulation we adopt the on-shell approximation for W and top quark (available as an option in the MCFM code), consistently with the electroweak calculation presented in this study. The input parameter values of the program have been tuned with the ones adopted in the electroweak calculation. For internal perturbative consistency we used in the NLO calculation the CTEQ6M set for PDFs. In addition, at NLO there is the need to fix the factorization and renormalization scales, $\mu_{\rm F}$ and $\mu_{\rm R}$, respectively. The typical way of studying the remaining QCD theoretical uncertainty of the predictions, as due to missing higher order terms, is to vary $\mu_{\rm F}$ and $\mu_{\rm R}$ around the relevant scale of the process, which, in the case under study, would be given by $m_t + m_W$. However, the presence of a b quark in the initial state introduces two subtleties, which have been addressed in [24]. The real $\mathcal{O}(\alpha_{\rm s})$ radiation contribution contains diagrams where an initial state gluon splits into a $b\bar{b}$ pair giving rise to the Wtb final state. The collinear $g \to b\bar{b}$ splitting is already accounted for in the b-quark distribution function, used in the lowest order calculation. Therefore the net contribution from the $gg \to Wtb$ diagrams should be approximately zero, including appropriate counter-terms and integrating over all b-quark transverse momenta up to $\mu_{\rm F}$. In [24] this has been checked to happen for $\mu_{\rm F} \leq 65\,\text{GeV}$. An additional problem associated with the $gg \to Wtb$ diagrams arises in the portion of the phase space where the Wb system crosses over the pole of the virtual top-quark propagator. Actually this contribution represents the doubly resonant $t\bar{t}$ production process, and it is preferable to exclude it from the NLO corrections to the tW process [24]. This is achieved in MCFM by applying a veto on the $p_{\rm T}$ of the additional b quark that appears at next-to-leading order. For consistency, the maximum allowed $p_{\rm T}$ of the b quark should be chosen to be of the same order of $\mu_{\rm F}$.

For the above reasons we have selected $\mu = \mu_{\rm F} = \mu_{\rm R} = 50\,\text{GeV}$ and $p_{\rm T}^{b\,\text{veto}} = 50\,\text{GeV}$, as in [24], and studied the

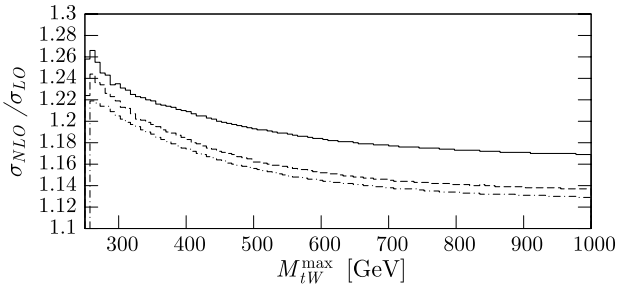

Fig. 5. QCD K-factor $(\sigma_{\rm NLO}(\mu)/\sigma_{\rm LO}\ \ (\mu_0 = 50\,\text{GeV}))$ as a function of $M_{tW}^{\rm max}$. The *solid line* is for $\mu = 25\,\text{GeV}$, the *dot-dashed line* for $\mu = 50\,\text{GeV}$, and the *dashed line* for $\mu = 100\,\text{GeV}$

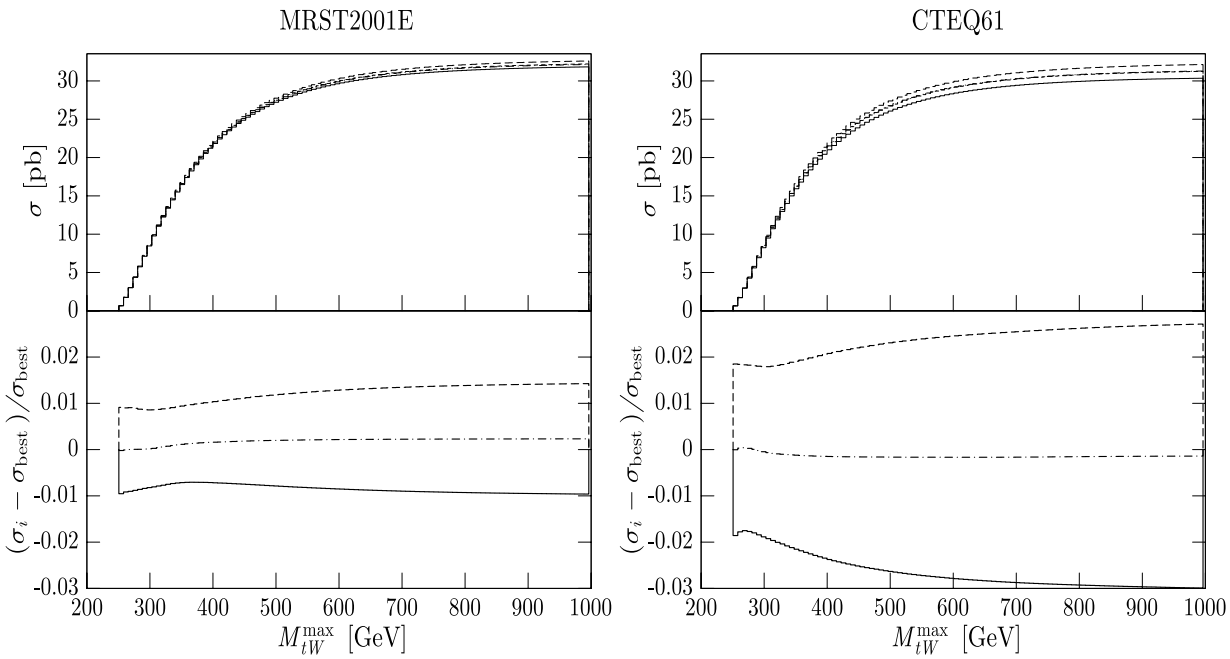

Fig. 6. *Left*: Integrated cross section from threshold up to $M_{tW}^{\rm max}$ (LO calculation) with the MRST2001E PDF set. For each bin, the minimum value (*solid line*), the maximum (*dashed*), the average (*dot-dashed*) and the value corresponding to the best fit parton density (*dotted*) are shown. In the *lower panel* the relative deviation with respect to the best fit PDF is shown. *Right*: the same as in the *left panel*, obtained with the set CTEQ61

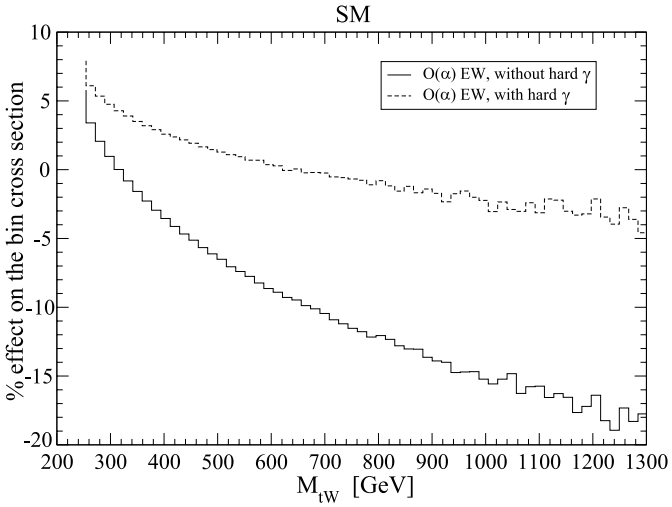

Fig. 7. The electroweak one-loop effect on the distribution $\mathrm{d}\sigma/\mathrm{d}M_{tW}$ in the standard model. The histogram "without hard photon" includes the soft-photon contributions only

variation of the resulting K-factor (defined as $\sigma_{\mathrm{NLO}}/\sigma_{\mathrm{LO}}$) in the range $25\,\mathrm{GeV} \leq \mu \leq 255\,\mathrm{GeV}$. The K-factor ranges from 1.26 for $\mu = 25\,\mathrm{GeV}$ to 1.12 for $\mu = 50$ and $100\,\mathrm{GeV}$ (1.17 for $\mu = 255\,\mathrm{GeV}$). The inclusive NLO cross section varies from $36.07(1)\,\mathrm{pb}$ for $\mu = 25\,\mathrm{GeV}$ to $34.84(1)\,\mathrm{pb}$ for $\mu = 50\,\mathrm{GeV}$, $35.09(1)\,\mathrm{pb}$ for $\mu = 100\,\mathrm{GeV}$ and $35.86(1)\,\mathrm{pb}$ for $\mu = 255\,\mathrm{GeV}$, thus showing stability at the level of few per cent, in agreement with Fig. 7 of [24].

At this point we can study the stability of the QCD NLO predictions on the partial rates. In Fig. 5, we quantify the size of the NLO QCD corrections showing the differential K-factor, with $p_{\mathrm{T}}^{b\,\mathrm{veto}} = 50\,\mathrm{GeV}$. The curves correspond to the values $\mu = 25$ (solid line), 50 (dot-dashed line) and 100 GeV (dashed line) in the NLO calculation, while the scale of the LO calculation is kept fixed at the value $\mu_0 = 50\,\mathrm{GeV}$. The size of the QCD corrections is of the order of 20%, decreasing by about 10% when M_{tW} ranges from threshold to 1 TeV. The scale uncertainties are lower than about 4%, being maximal at the highest M_{tW}.

4.2 SUSY QCD corrections

The one-loop SUSY QCD effects on the three channels of single top production have been computed at LHC in [15]. These are radiative corrections with propagation of virtual gluinos in the quantum loop. The numerical analysis of [15] is performed in the constrained MSSM within mSUGRA. The MSSM parameters are the five inputs at grand unification scale

$$M_{1/2}\,,\ M_0\,,\ A_0\,,\ \tan\beta\,,\ \mathrm{sign}\,\mu\,, \qquad (2)$$

where $M_{1/2}, M_0, A_0$ are the universal gaugino mass, scalar mass, and the trilinear soft breaking parameter in the superpotential. This last parameter has been set to $A_0 = -200\,\mathrm{GeV}$. The sign of μ is positive.

The effects in the associated production channel are studied by evaluating the K-factor defined as the ratio of the SUSY QCD corrected cross sections to LO total cross sections, calculated using the CTEQ6M PDFs set. The dependence of the K-factor on the various MSSM parameters is analyzed in great detail.

The dependence on the gluino mass $M_{\tilde{g}}$ ($M_{1/2}$) can be studied at various values of $\tan\beta = 5$, 20 and 35. The K-factor increases with $M_{\tilde{g}}$ for small $M_{\tilde{g}}$ ($\lesssim 160\,\mathrm{GeV}$), while it decreases with $M_{\tilde{g}}$ for large $M_{\tilde{g}}$ ($\gtrsim 160\,\mathrm{GeV}$). In general the dependence on $\tan\beta$ is rather mild. The typical values are about $K = 1.06$.

For example, assuming $\tan\beta = 5$ and computing the K-factor as functions of $M_{\tilde{g}}$ ($M_{1/2}$) for different M_0, one finds that there are large variations in K when $M_{\tilde{g}}$ becomes small. It decreases with $M_{\tilde{g}}$ and especially rapidly when $M_{\tilde{g}} \lesssim 150\,\mathrm{GeV}$ at least for $M_0 = 150\,\mathrm{GeV}$. Nevertheless, as soon as $M_{\tilde{g}}$ becomes large, the decoupling of heavy gluinos ($M_{\tilde{g}} \gtrsim 450\,\mathrm{GeV}$) gives saturated stable values of K. Again $K \simeq 1.06$ for $M_{\tilde{g}} \lesssim 500\,\mathrm{GeV}$.

Similar results are obtained by varying the stop mass $M_{\tilde{t}_1}$ (M_0), assuming $\tan\beta = 5$, and $M_{1/2} = 40$, 70 and

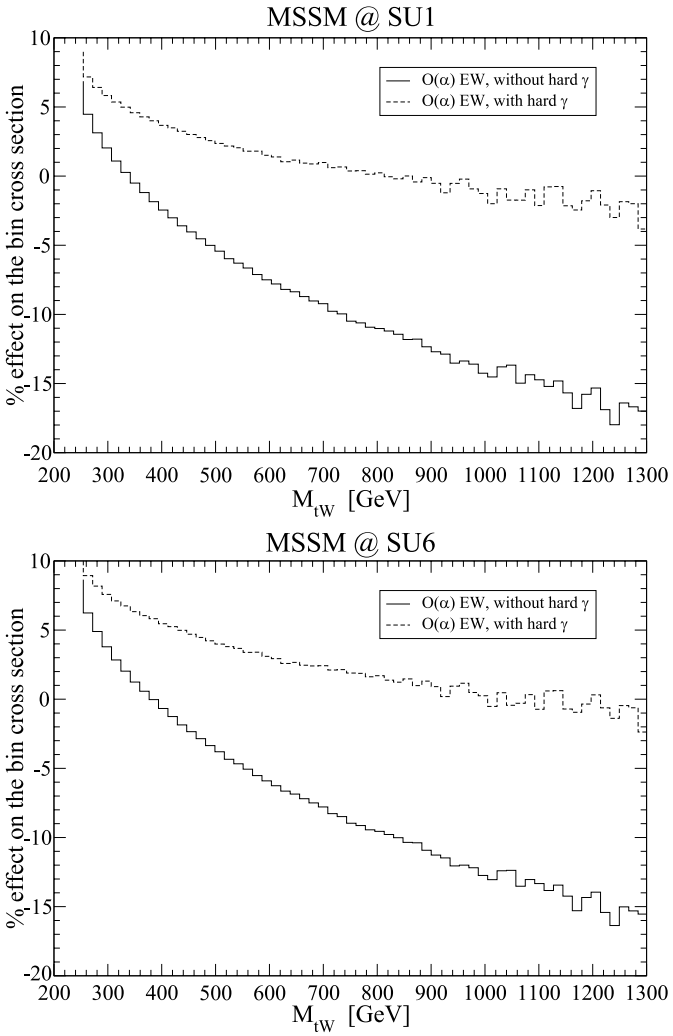

Fig. 8. The electroweak one-loop effect on the distribution $\mathrm{d}\sigma/\mathrm{d}M_{tW}$ in the MSSM at the two benchmark points SU1 and SU6

100 GeV, respectively. The K-factor is about 1.06 for most values of $M_{\tilde{t}_1}$, decreasing slowly with $M_{\tilde{t}_1}$.

In conclusion, the typical SUSY QCD correction to the process of associated production is about +6% for most values of the explored parameter values.

4.3 PDF uncertainties

Another source of theoretical uncertainty is given by the contribution of the parametric errors associated with the parton densities. This could become particularly relevant for single top channels, due to the presence of an initial state b quark, whose distribution function is strictly related to the gluon distribution. We have studied the impact of such uncertainties by using the NLO PDF sets MRST2001E and CTEQ61 as in the LHAPDF package [26, 27]. The results are shown in Fig. 6. The spread of the predictions obtained with the MRST set displays a relative deviation of about 1%, while the CTEQ set gives a larger uncertainty reaching the 3% level for high tW mass. This is due to different values of the tolerance parameter [28, 29], the latter being defined as the allowed maximum of the $\Delta\chi^2$ variation with respect to the parameters of the best PDFs fit. Conservatively, we can associate to our predictions an uncertainty due to the present knowledge of parton densities of about 3%. However, it is worth noting that the uncertainties obtained according to such a procedure are of purely experimental origin only (i.e. as due to the systematic and statistical errors of the data used in the global fit), leaving aside other sources of uncertainty of theoretical origin.

5 Results

Coming back to the genuine electroweak corrections, we present in this section our results for the distribution $\mathrm{d}\sigma/\mathrm{d}M_{tW}$ and for the integrated cross section in the standard model and in the MSSM. The numerical results shown in the following have been obtained in terms of the LO PDF set CTEQ6L with $\mu = m_t + M_W$, the latter being the top-quark and W-boson mass, respectively.

We begin with the invariant mass distribution $\mathrm{d}\sigma/\mathrm{d}M_{tW}$. We show in Fig. 7 the electroweak effect in the standard model case. The two lines allow one to appreciate the effect of the hard photon radiation. It adds a positive contribution to the effect that is uniformly positive over most of the explored energy range. The effects in the MSSM are shown in Fig. 8 at the two benchmark points SU1 and SU6. The pattern is similar to that of the standard model, in agreement with the general partial decoupling of the genuine SUSY components.

The behaviour of the integrated cross section is shown in Fig. 9 for the standard model, and in Fig. 10 for the MSSM. Again, the pattern is similar. The cross section is integrated from threshold up to a maximum invariant mass $M_{tW}^{\max}$. The electroweak effect is always positive and is maximum for small $M_{tW}^{\max}$. This is a consequence of a coherent sum of positive one-loop effects coming from the electroweak sector of the MSSM and from the complete QED contribution. For larger tW invariant masses, the electroweak SM contribution decreases, and the overall effect is weakened. For what concerns the electroweak SUSY effect, it remains of the order of a few (positive) percent in all the considered benchmark points, the largest effect being obtained in the SU6 case. This is not, though, the total genuine SUSY effect. In fact, to obtain the latter, one still has to add the SUSY QCD contribution of [15]. The corresponding effect on the integrated partial rates is shown by the dashed curves in the right panels of Fig. 10 in a qualitative, but essentially correct, way, simulating the SUSY QCD component by a constant 6% shift, consistently with the analysis of [15]. From an inspection of

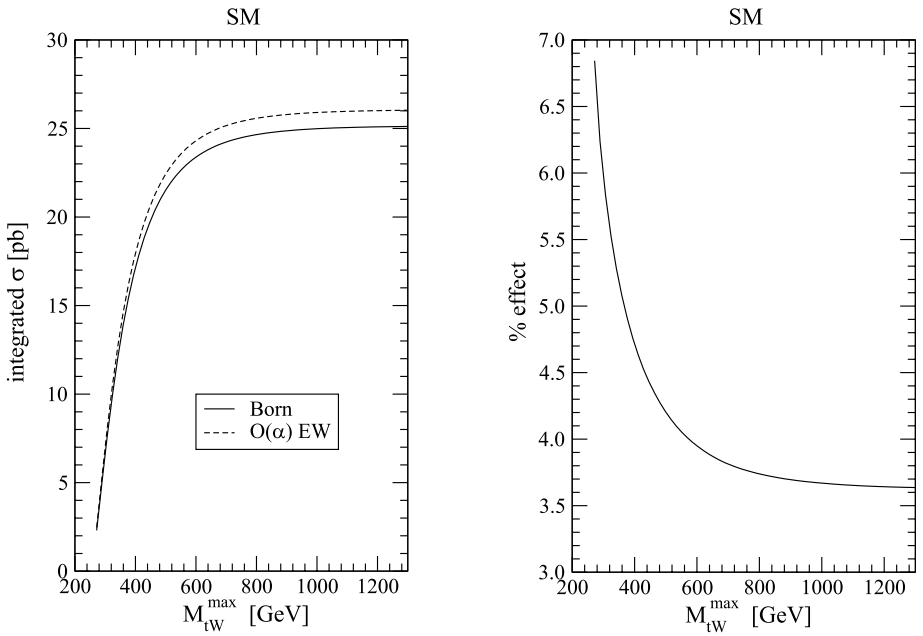

Fig. 9. Integrated cross section (from threshold up to $M_{tW}^{\max}$) and electroweak one-loop effect in the standard model

Fig. 10 one can conclude that, for final invariant masses of the 400 GeV size, an overall one-loop effect of approximately 13%–14% is produced in the MSSM by the positive sum of electroweak and SUSY QCD contributions. The size of the genuine one-loop SUSY effect is of roughly the order of ten percent. To obtain the complete value of the rates it is now sufficient to add to the values of Fig. 10 the remaining SM QCD effect, exhaustively illustrated in Sect. 4. In this way, the complete one-loop expression of the rates can be obtained. In fact, from the calculations that we have performed, the values of other possibly interesting observable quantities can be easily obtained. The reason why we have limited our presentation to the partial rates will be summarized in the final conclusions.

6 Conclusions

We have performed in this paper the first (to our knowledge) complete calculation of the one-loop effect on the process of tW production, including a discussion of the overall size of the theoretical uncertainties. Our interest has been concentrated on the particular quantities that we have defined as partial rates, with special emphasis on the low (400 GeV) final invariant mass. The reason of this interest is actually twofold, since with this choice the related quantity meets, at the same time, two conditions on the purely theoretical side. In fact, it maximizes the overall one-loop electroweak (including QED) effect, which can reach the 8% size, a value that should not be neglected.

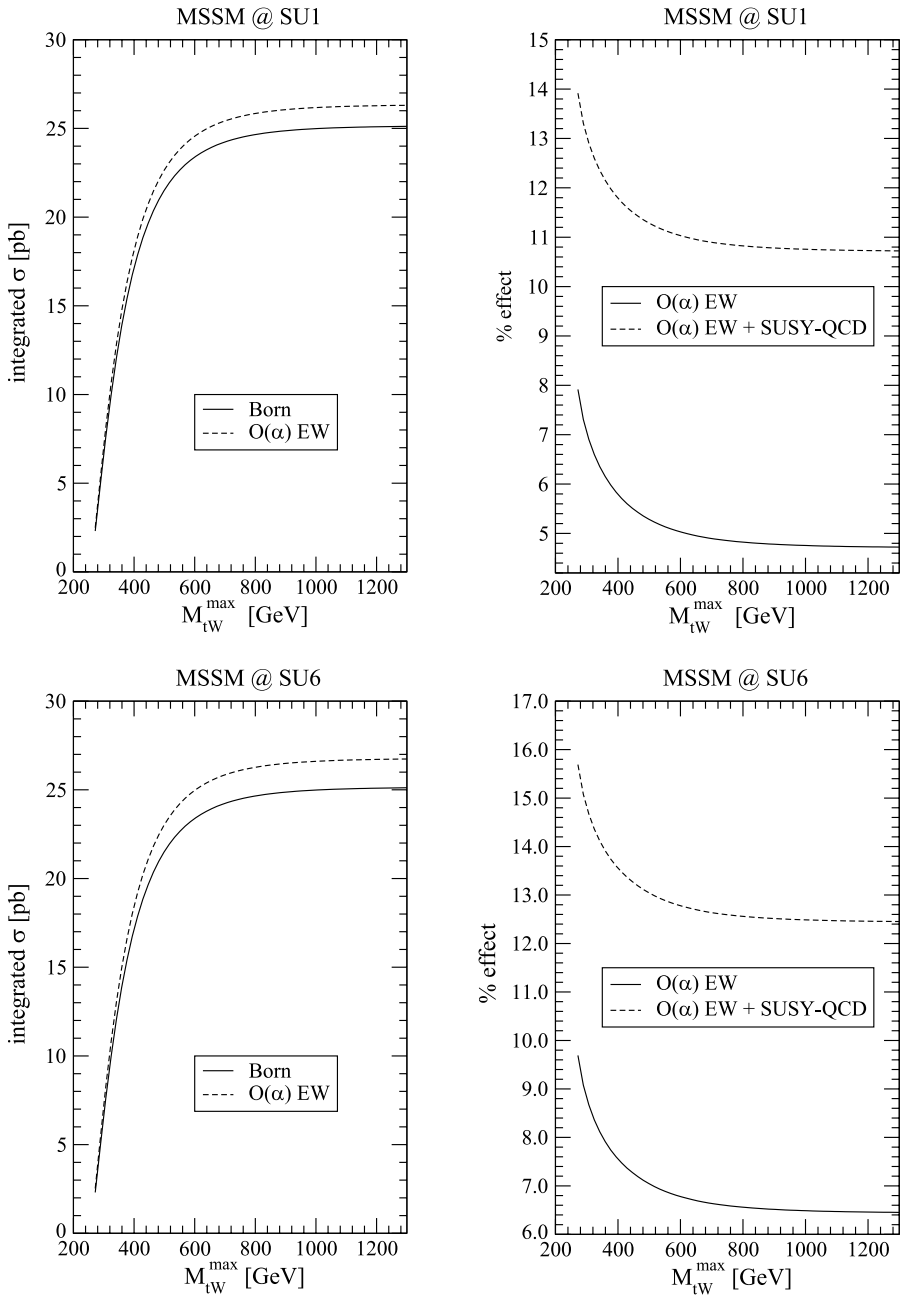

Fig. 10. The integrated cross section (from threshold up to $M_{tW}^{\max}$) and electroweak one-loop effect in the MSSM at the two benchmark points SU1 and SU6. SUSY QCD corrections have been inserted in the *dashed line* of the *right panel* and simulated by a +6% shift, consistently with the analysis of [15]

With the addition of SUSY QCD one-loop terms, the genuine SUSY contribution reaches the 10% size. At the same time, it minimizes the theoretical uncertainties that we have considered in the paper. On the purely experimental side, we do not have yet at our disposal a rigorous experimental analysis of the tW production process, which seems to us extremely relevant and necessary. It is well known that the largest background for associated tW production is top-quark pair production. From the point of view of signal identification, the region with small tW invariant mass, near the $t\bar{t}$ threshold, has possibly a chance to be optimal. Waiting for a dedicated effort we can though rely on the fact that a measurement of the rate at the ten percent level should be considered as a "must" project for the study of single top production. Should this result be met, the measurement of our partial rates could indeed represent a relevant and original test of genuine SUSY effects in the MSSM at LHC.

Acknowledgements. We are grateful to Marina Cobal for discussions. The work of C.M. Carloni Calame is supported by a Royal Society and British Council Short Visit grant.

References

1. W. Wagner, Rep. Prog. Phys. **68**, 2409 (2005) [hep-ph/0507207]
2. T.M.P. Tait, Phys. Rev. D **61**, 034001 (2000) [hep-ph/9909352]
3. M. Beneke et al., in Proc. of the Workshop on Standard Model Physics (and more) at the LHC, ed. by G. Altarelli, M.L. Mangano, CERN 2000-004, Geneva 2000, p. 419
4. ATLAS Detector and Physics Performance Technical Design Report, CERN/LHCC 99-14/15
5. CMS Physics Technical Design Report, Vol. II: Physics Performance, CERN/LHCC 2006/021
6. G. Bordes, B. van Eijk, Nucl. Phys. B **435**, 23 (1995)
7. M.C. Smith, S. Willenbrock, Phys. Rev. D **54**, 6696 (1996) [hep-ph/9604223]
8. T. Stelzer, Z. Sullivan, S. Willenbrock, Phys. Rev. D **56**, 5919 (1997) [hep-ph/9705398]
9. B.W. Harris, E. Laenen, L. Phaf, Z. Sullivan, S. Weinzierl, Phys. Rev. D **66**, 054024 (2002) [hep-ph/0207055]
10. Z. Sullivan, Phys. Rev. D **70**, 114012 (2004) [hep-ph/0408049]
11. J. Campbell, R.K. Ellis, F. Tramontano, Phys. Rev. D **70**, 094012 (2004) [hep-ph/0408158]
12. Q.-H. Cao, C.-P. Yuan, Phys. Rev. D **71**, 054022 (2005) [hep-ph/0408180]
13. Q.-H. Cao, R. Schwienhorst, C.-P. Yuan, Phys. Rev. D **71**, 054023 (2005) [hep-ph/0409040]
14. Q.-H. Cao, R. Schwienhorst, J.A. Benitez, R. Brock, C.-P. Yuan, Phys. Rev. D **72**, 094027 (2005) [hep-ph/0504230]
15. J.J. Zhang, C.S. Li, Z. Li, L.L. Yang, Phys. Rev. D **75**, 014020 (2007) [hep-ph/0610087]
16. M. Beccaria, G. Macorini, F.M. Renard, C. Verzegnassi, Phys. Rev. D **73**, 093001 (2006) [hep-ph/0601175]
17. M. Beccaria, G. Macorini, F.M. Renard, C. Verzegnassi, to appear in the Proc. of the Workshop Flavour in the Era of the LHC, 2007
18. ATLAS Data Challenge 2 DC2 points, http://paige.home.cern.ch/paige/fullsusy/romeindex.html
19. J.A.M. Vermaseren, math-ph/0010025
20. G. 't Hooft, M. Veltman, Nucl. Phys. B **153**, 365 (1979)
21. W.T. Giele, S. Keller, E. Laenen, Phys. Lett. B **372**, 141 (1996) [hep-ph/9511449]
22. S. Zhu, Phys. Lett. B **524**, 283 (2002) [hep-ph/0109269]
23. S. Zhu, Phys. Lett. B **537**, 351 (2002) [Erratum]
24. J. Campbell, F. Tramontano, Nucl. Phys. B **726**, 109 (2005) [hep-ph/0506289]
25. J. Campbell, R.K. Ellis, http://mcfm.fnal.gov/
26. http://hepforge.cedar.ac.uk/lhapdf/
27. M.R. Whalley, D. Bourilkov, R.C. Group, hep-ph/0508110 and references therein
28. A.D. Martin, R.G. Roberts, W.J. Stirling, R.S. Thorne, Eur. Phys. J. C **28**, 455 (2003) [hep-ph/0211080]
29. J. Pumplin, D.R. Stump, J. Houston, H.L. Lai, P. Nadolsky, W.K. Tung, JHEP **0207**, 012 (2002) [hep-ph/0201195]